^{27}Al NMR studies of itinerant electron ferromagnetic Ni_3AlC_x

Bin Chen,* Hiroto Ohta, Chishiro Michioka, Yutaka Itoh, and Kazuyoshi Yoshimura†
Department of Chemistry, Graduate School of Science, Kyoto University, Kyoto 606-8502, Japan
(Received 10 December 2009; revised manuscript received 17 March 2010; published 13 April 2010)

Carbon-intercalation effects on weakly ferromagnetic Ni_3Al have been studied by ^{27}Al spin-echo NMR techniques. The Knight shift K and the nuclear spin-lattice relaxation time T_1 of ^{27}Al have been measured in the carbon-intercalated Ni_3AlC_x with $x=0$, 0.01, 0.02, 0.05, and 0.1, whose Curie temperatures are 36 K, 18 K, <2 K, <2 K and <2 K, respectively. The magnitude of the negative ^{27}Al hyperfine coupling constants were found to decrease at first, and then increase with the carbon intercalation into the body-center site of Ni_3Al. The linear relations between the $1/T_1T$ and the magnetic susceptibility χ indicate that the three-dimensional ferromagnetic spin fluctuations are dominant in the Ni_3AlC_x system. We estimate the evolution of the characteristic temperature of spin fluctuations, T_0, in frequency space when the system changes from weak ferromagnetism to a nearly ferromagnetic state. Then, we analyze the temperature dependence of inverse magnetic susceptibilities and discuss the feature of the spin fluctuations in this system. As a result, the carbon-intercalation effect was found to be over a long range, inducing three-dimensional ferromagnetic quantum phase transition at $x \sim 0.02$.

DOI: 10.1103/PhysRevB.81.134416 PACS number(s): 75.40.Gb, 75.50.Cc

I. INTRODUCTION

Magnetic quantum phase transition and the associated quantum critical behavior have been studied extensively in some correlated electron systems. Compared with the 4f-electron compounds, 3d-transition-metal compounds have seldom been studied recently in details.[1,2] Among them, there have been still several reports on nearly or weakly ferromagnetic materials such as MnSi,[3] Ni_3Al,[4] FeGe,[5] and $ZrZn_2$.[6,7] The physical properties of these materials, such as electrical conductivity, magnetism, etc., are well interpreted in the frame of the self-consistent renormalization (SCR) theory of spin fluctuations developed by Moriya and co-workers.[8] Therein, the magnetic spin fluctuations play an important role in determining the physical properties of these materials. Furthermore, in the SCR theory, the nature of the spin-fluctuation spectrum is characterized directly by two important parameters, T_0 and T_A, which characterize the widths of the spin-excitation spectrum in frequency ω and momentum q spaces, respectively.[8] Here, we can estimate them from the results of experiments such as magnetization measurements, neutron scattering, and NMR relaxation measurements.[9–11] Therefore, the feature of spin fluctuations has been studied intensively in various systems and the quantitative agreements between the experiments and theoretical calculations have been found to be very well, thus far.[10,12,13] However, the influence of an external parameter, such as external physical pressure, chemical substitution, etc., on the spin-fluctuation spectrum has hardly been studied systematically up to now.[13,14] Therefore, it is very important to study the evolution of the spin-fluctuation spectrum for a system from magnetic ordered state to the paramagnetic state crossing the quantum critical point (QCP) for a fully understanding of the 3d itinerant magnetism.

Among these itinerant ferromagnets, now we are very interested in the Ni_3Al system, which is a typical weak itinerant ferromagnet with the cubic Cu_3Au structure.[15] Ni atoms are at the face-centered position of each cubic unit cell, where Al atoms are situated at the corner site of each cube. The Curie temperature T_C can be suppressed to zero at the critical $P_c=80$ kbar for Ni_3Al under pressure[4] and at the critical concentration $x_c=0.10$ for $(Ni_{1-x}Pd_x)_3Al$ upon substitution.[16] The electrical resistivity measurements indicate that the three-dimensional spin fluctuations are dominant in this system. Recently, the magnetic measurements on the carbon-intercalated Ni_3AlC_x showed that the magnetic long-range order is suppressed by the carbon intercalation.[17–19] The theoretical calculation suggested that this may be due to the hybridization between Ni 3d and C 2p orbitals.[20,21] Our magnetic measurements show that the spin fluctuations of the itinerant electrons are dominant in describing the magnetic properties in this system, and the carbon intercalation leads to the modification of the electronic state near the Fermi surface, which results in the drastic change in the magnetism through the QCP.[19] The systematic changes in the electronic states and the magnetic spin-fluctuation spectrum in this system have still been unclear so far.

Since the nuclear magnetic resonance (NMR) is a local probe of electronic spins through hyperfine interactions, it is useful to understand the microscopic characteristics of electronic systems, including the spin dynamics of the magnetic materials. In this paper, we report a systematic ^{27}Al NMR study of Ni_3AlC_x with the carbon intercalation of $x=0$, 0.01, 0.02, 0.05, and 0.1. Our results indicate that the ferromagnetic spin fluctuations play an important role in determining the magnetic properties of Ni_3AlC_x from the ferromagnetic to paramagnetic states.

II. EXPERIMENTS

The polycrystalline samples of Ni_3AlC_x (nominal concentration $x=0$, 0.01, 0.02, 0.05, and 0.1) were synthesized by the arc-melting method in an atmosphere of high-purity argon gas (99.99%). Starting materials used in this study were

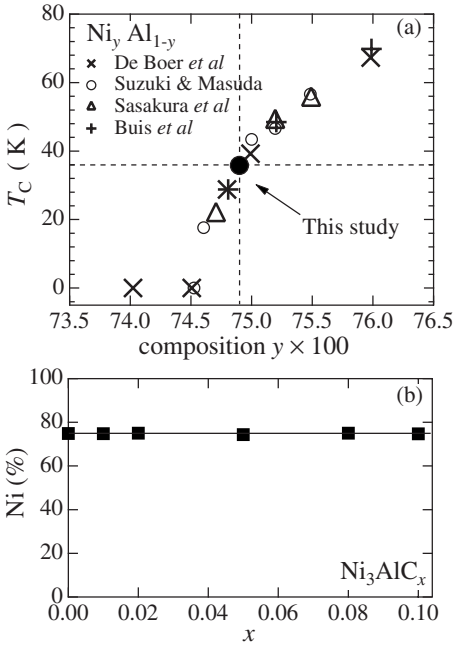

FIG. 1. (a) Ni composition-y dependence of the Curie temperature T_C for Ni_yAl_{1-y}. The plotted data of the Curie temperatures are reproduced from the former papers by de Boer *et al.* (Ref. 22), Suzuki and Masuda (Ref. 23), Sasakura (Ref. 15), and Buis *et al.* (Ref. 24). (b) Ni concentrations for Ni_3AlC_x with x=0, 0.01, 0.02, 0.05, 0.08, and 0.1.

99.9% pure Ni ingot, 99.99% Al ingot, and 99.8% carbon sheet. The melting was repeated at least six times to ensure the homogeneity. The arc-melted buttons were annealed at 1050 °C for 1 week in evacuated quartz tubes. No obvious weight loss was found during the above process. After that the annealed buttons were cut to small pieces of about 50 mg by a diamond cutter. To remove the disorder in the samples introduced through the mechanical treatments, these pieces were annealed again with the same condition as described above for 3 days.

For Ni_3Al system, its magnetic properties are very sensitive to nickel composition.[22] The Ni composition dependence of the Curie temperatures of Ni_yAl_{1-y} is shown in Fig. 1(a). So it is important to verify the final composition of samples. We determine the Ni concentration for each sample with energy-dispersive x-ray spectroscopy (EDS). Because the carbon composition can hardly be determined by EDS, we only determine the relative compositions of Ni and Al. As shown in Fig. 1(b), the Ni concentrations are about $74.9 \pm 0.1\%$ for all the samples. Furthermore, we found the plot of our data of T_C (36 K) (Ref. 19) vs y (74.9%) is in a good agreement with the previously reported phase diagram in Fig. 1(a),[15,22–24] resulting in the good reliability of our EDS analyses. Thus, hereafter we represent the sample name only as Ni_3AlC_x in this study.

The x-ray diffraction (XRD) pattern was collected with Cu $K\alpha$ radiation at room temperature. The XRD patterns of Ni_3AlC_x shown in Fig. 2 indicate that all the samples are in a single phase of the Cu_3Au structure. The samples are too ductile to be crushed into powders. Therefore, the XRD patterns were measured with the bulk samples. Some crystal

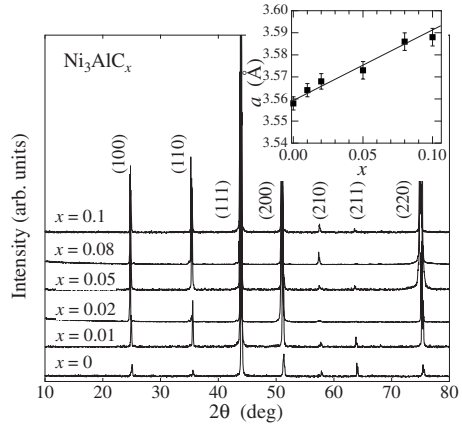

FIG. 2. X-ray diffraction pattern for Ni_3AlC_x at room temperature. The inset shows the x dependence of the lattice constant a.

planes may align along the bulk surface leading to the emphasis of the diffraction intensity due to this plane. As a result, pattern intensities differ from those of the powder pattern. Here, peak intensity ratio does not show consistency with x. On the other hand, the relatively large error of 2θ is usually obtained at low angle range. Therefore, we use the extrapolation method to refine the lattice parameters, i.e., we obtain the lattice parameters from the a vs $\sin^2\theta$ plot with 2θ extrapolated to 180°. The inset of Fig. 2 shows the carbon-concentration dependence of the lattice constant a. The slightly increase in a with increasing carbon concentration x may be ascribed to the carbon intercalation into the body-center site of Ni_3Al. As shown latter, the systematic changes in magnetic properties of Ni_3AlC_x can be ascribed to this carbon-intercalation effects.

The magnetization measurements were performed using a superconducting quantum interference device (SQUID) magnetometer in the temperature range from 2 to 300 K with applied magnetic fields H up to 5 T. For the observation of ^{27}Al NMR signals (nuclear spin $I=5/2$, the nuclear gyromagnetic ratio $^{27}\gamma/2\pi=11.094$ MHz/T), a phase-coherent pulsed NMR spectrometer was utilized. The NMR frequency spectra were obtained by plotting the spin-echo intensity vs frequency. The external magnetic field used for the NMR measurements was fixed to $H=7.4847$ T.

III. RESULTS AND DISCUSSION

A. Magnetic susceptibility

Figure 3(a) shows the temperature dependence of inverse magnetic susceptibilities $\chi^{-1}(\equiv H/M)$ of Ni_3AlC_x (x=0, 0.01, 0.02, 0.05, 0.08, and 0.1). The Curie-Weiss (CW) behavior was observed for all the samples in the high-temperature region. The x dependence of the Weiss temperature θ (estimated from the CW fit of χ) and the Curie temperature T_C (determined from the Arrott plots, i.e., M^2 vs H/M plots)[19] are shown in Fig. 3(b). The ferromagnetic long-range ordering was completely suppressed at about x =0.02: the T_C approaches to zero at about x=0.02, and the sign of the Weiss temperature θ changes from positive to negative around x=0.04.

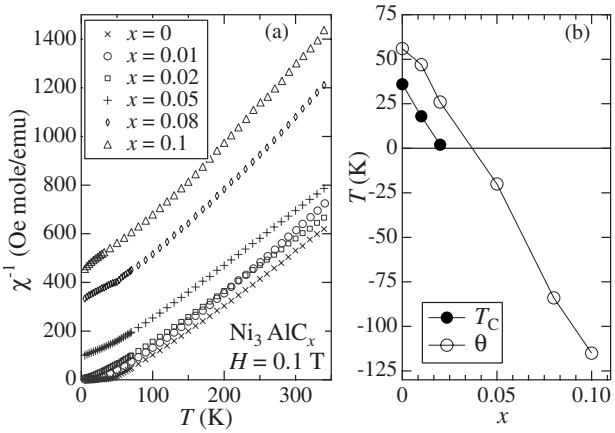

FIG. 3. (a) Temperature dependences of inverse magnetic susceptibilities χ^{-1} for Ni_3AlC_x (x=0, 0.01, 0.02, 0.05, 0.08, and 0.1) measured at magnetic field of H=0.1 T. (b) The x dependence of the Curie temperature T_C and the Weiss temperature θ.

B. Knight shift and hyperfine coupling constant

Figure 4 shows the frequency-swept ^{27}Al NMR spectra at several temperatures for Ni_3AlC_x with x=0.01, 0.02, and 0.1 in the external magnetic field of H=7.4847 T. Near the room temperature, we found that the linewidths of spectra for x=0, 0.01, and 0.02 are almost the same, and found the slight broadenings of the spectra for x=0.05 and 0.1. On the other hand, with decreasing temperature, the ^{27}Al NMR spectra were observed to be broadened very much for all the samples. Below 100 K, the NMR linewidths for x=0, 0.01, and 0.02 were much larger than those for x=0.05 and 0.1. Usually, the two origins of broadening should be considered through the magnetic and the quadrupole interaction. Since the ^{27}Al nuclei are at the cubic sites, a broadening due to the quadrupole interaction is not expected. However, because of the carbon intercalation will lead to the local distortion of the lattice, the broadening due to the quadrupole interaction may be expected. With the increase in the carbon concentration, the local quadrupole interaction will be dominant at high temperatures. This may be the reason for the broadening of

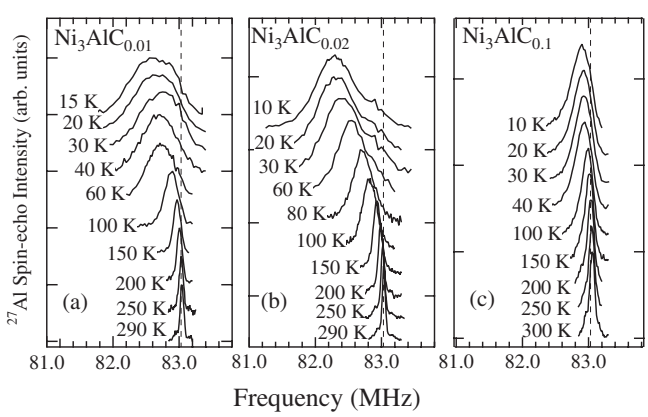

FIG. 4. Frequency-swept ^{27}Al NMR spectra of Ni_3AlC_x (x =0.01, 0.02, and 0.1) at the external magnetic field of H =7.4847 T. The dotted lines show the zero Knight shift ^{27}K=0 for ^{27}Al.

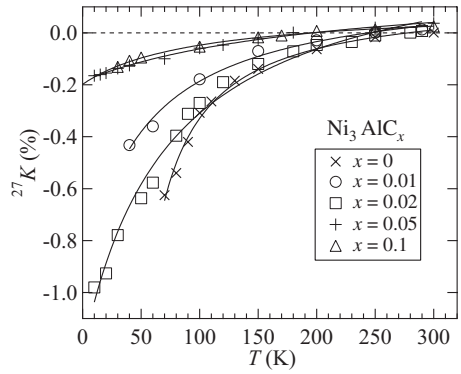

FIG. 5. Temperature dependence of ^{27}Al Knight shift ^{27}K of Ni_3AlC_x (x=0, 0.01, 0.02, 0.05, and 0.1).

the spectra with x=0.05 and 0.1 near room temperature. We should note that the large increases in linewidths of the spectra with decreasing temperature cannot be explained by the quadrupole interaction. Therefore, this kind of broadening may arise from magnetic interaction, such as the inhomogeneous distribution in magnitude of the magnetic moment of the Ni atom.[25]

Figure 5 shows the temperature dependence of ^{27}Al Knight shift ^{27}K. The magnitudes of Knight shifts are estimated from the peak frequencies of the ^{27}Al NMR spectra as shown in Fig. 4. The Knight shifts ^{27}K show the CW-type temperature dependence and decrease monotonically with decreasing temperature. In Fig. 6, the Knight shifts ^{27}K for all the samples are plotted against the uniform magnetic susceptibility $\chi \equiv M/H$ with temperature as an implicit parameter. The uniform magnetic susceptibilities used here were measured by a SQUID with a magnetic field of 4.5 T.

Usually, for the d-band metals, the bulk magnetic susceptibility χ can be decomposed into several components as

$$\chi(T) = 3\chi_d(T) + 3\chi_{orb} + \chi_s + \chi_{dia}, \quad (1)$$

where $\chi_d(T)$ and χ_{orb} are the spin and orbital susceptibilities of d electrons per Ni atom, χ_s is the spin susceptibilities of s and p conduction electrons, and χ_{dia} is the diamagnetic susceptibilities of core electrons. Only χ_d can be assumed to

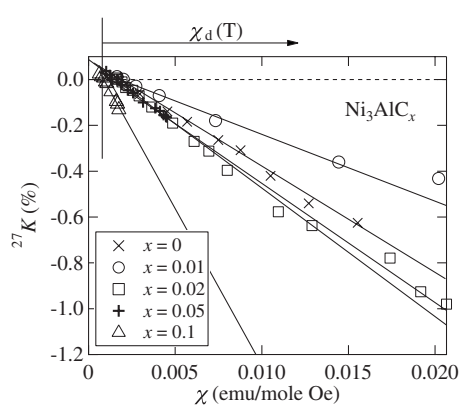

FIG. 6. ^{27}Al Knight shift ^{27}K plotted against magnetic susceptibility with temperature as an implicit parameter (K-χ plot) of Ni_3AlC_x (x=0, 0.01, 0.02, 0.05, and 0.1).

TABLE I. The ^{27}Al hyperfine coupling constant of the Ni_3AlC_x.

x	A_{hf} (kOe/μ_BNi)
0	−7.8
0.01	−5.0
0.02	−8.7
0.05	−9.4
0.1	−22.8

depend on temperature. The linear relations in the K-χ plots as seen in Fig. 6 indicate that the microscopic susceptibilities at the Al site is governed by the bulk susceptibility originating from the Ni 3d electrons. Furthermore, ^{27}Al nuclei can be thought to see only the hyperfine fields transferred from Ni 3d spins through the conduction-electron bands and/or d-p-band hybridizations. Therefore, this field which ^{27}Al sees is so called the transferred hyperfine field. Thus, the temperature-dependent part of the ^{27}Al Knight shift originates from Ni $\chi_d(T)$ and given by

$$^{27}K(T) \approx \frac{A_{hf}}{N_A \mu_B}\chi_d(T), \tag{2}$$

where N_A is Avogadoro's number and μ_B the Bohr magneton. The ^{27}Al hyperfine coupling constants A_{hf} estimated from the slops of the K-χ plots are listed in Table I. For Ni_3Al, our result is almost the same as that reported before.[25] It was found that the magnitude of hyperfine coupling constant A_{hf} decreases first and then increases with the increase in carbon intercalation x. Here, the transferred hyperfine fields at the ^{27}Al site away from the carbons are thought to be modified by the intercalated carbon as well. The carbon intercalation may cause carrier doping effects but may not bring local impurity effects. For all the samples, the hyperfine coupling constants A_{hf}'s are negative. Since $^{27}A_{hf}$ is isotropic, the dipole field from Ni moments is not predominant at the Al site. The core polarization due to the Al 3p electrons is also excluded because it should give a positive value of the hyperfine coupling constant.[26] In order to explain the negative value, an exchange-polarization-transfer mechanism to an empty orbital of the Ni ion might be considered.[27] The magnitude of A_{hf} for x=0.1 is three times larger in magnitude than that of the pure Ni_3Al.

C. Nuclear spin-lattice relaxation rate $1/T_1$

Figure 7(a) shows the temperature dependence of the ^{27}Al nuclear spin-lattice relaxation rate $1/T_1$ for Ni_3AlC_x with x =0, 0.01, 0.02, 0.05, and 0.1. The T_1 was measured at the peak frequency of the NMR spectrum, and determined by fitting the recovery curve to a single exponential function $\propto\exp(-\frac{t}{T_1})$. The observed $1/T_1$ decreases monotonically with decreasing temperature but does not follow a simple Korringa relation ($1/T_1 \propto T$). In Fig. 7(b), we present the temperature dependence of the ^{27}Al nuclear spin-lattice relaxation rate $1/T_1$ divided by temperature T, $1/T_1T$.

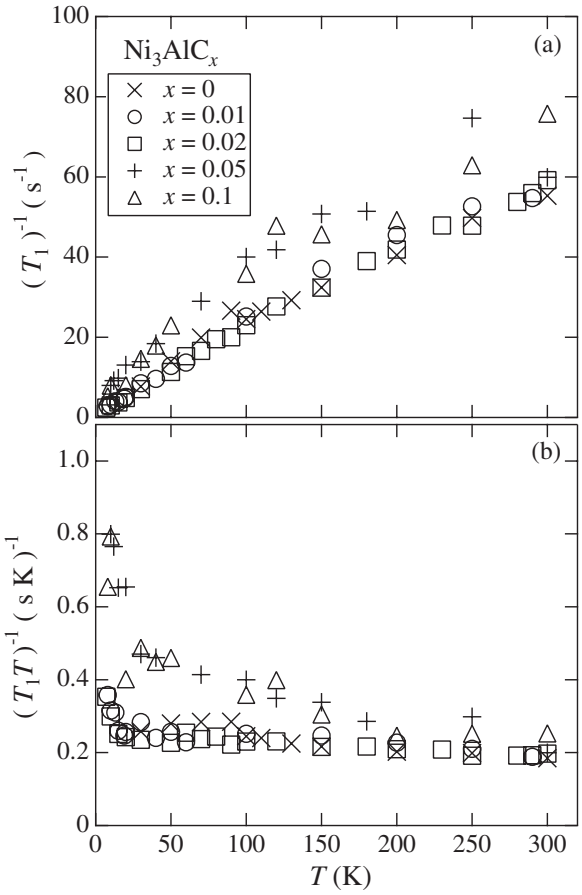

FIG. 7. (a) Temperature dependence of the nuclear spin-lattice relaxation rate $1/T_1$ of ^{27}Al of Ni_3AlC_x with x=0, 0.01, 0.02, 0.05, and 0.1 measured at the external magnetic field H=7.4847 T. (b) The corresponding temperature dependence of $1/T_1T$ for each sample.

In general, $1/T_1T$ can be written as the wave-vector q summation of the imaginary part of the dynamical electronic susceptibility $\chi''(q,\omega_n)$ as[8]

$$\frac{1}{T_1T} = \frac{\gamma_n^2 k_B}{\mu_B^2 \hbar}\sum_q |A_{hf}(q)|^2 \frac{\chi''(q,\omega_n)}{\omega_n}, \tag{3}$$

where $A_{hf}(q)$ is the q-dependent hyperfine coupling constant and ω_n the NMR frequency.

For Ni_3Al, i.e., x=0, compared with the result of Uemura *et al.*,[25] the peak of $1/T_1T$ near T_C, which originates from critical ferromagnetic spin fluctuations, was almost suppressed by the strong magnetic field of H=7.4847 T applied in the present experiment, and only a slight temperature dependence of $1/T_1T$ was observed as seen in Fig. 7(b). With the same reason, we might believe that the spin fluctuations are suppressed for x=0.01, 0.02, 0.05, and 0.1 samples as well. However, for x=0.05 and 0.1, the $1/T_1T$ data show monotonic increases and large enhancements in their magnitudes with the decrease in temperature, indicating that the low-frequency spin fluctuations are greatly enhanced in the case of x=0.05 and 0.1. These results are quite different from the x dependence of the uniform susceptibility $\chi(q=0,\omega$

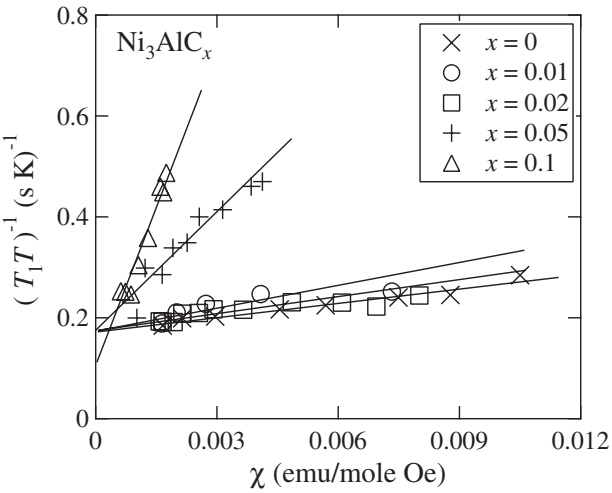

FIG. 8. $1/T_1T$ of Ni_3AlC_x (x=0, 0.01, 0.02, 0.05, and 0.1) plotted against the susceptibility χ with the temperature as an implicit parameter.

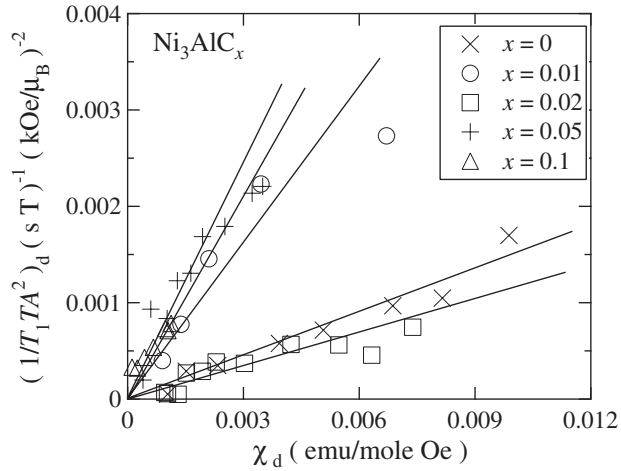

FIG. 9. $(1/T_1TA^2)_d$ of Ni_3AlC_x (x=0, 0.01, 0.02, 0.05, and 0.1) plotted against the d-electron part of susceptibility χ_d with the temperature as an implicit parameter.

=0), where the uniform susceptibility is suppressed with the carbon intercalation. As shown in Eq. (3), $1/T_1T \propto \Sigma_q A_{hf}(q)^2\chi''(q,\omega_n)/\omega_n$, the three-dimensional ferromagnetic fluctuations are dominant in these samples. Furthermore, for x=0.05 and 0.1, the enhancement of $1/T_1T$ can be ascribed to not only the increase in the hyperfine coupling constant A_{hf} but also the strongly enhanced spin fluctuations in these samples.

In order to obtain the information about spin-fluctuation character, the comparison between $1/T_1T$ and Knight shift (or χ) are necessary. If antiferromagnetic (AFM) correlations are dominant, the dynamical susceptibility has peaks at the AFM wave vector Q apart from q=0, i.e., $q=\pi$, therefore $1/T_1T$ is mainly dominated by $\chi(Q)$. In contrast, when ferromagnetic correlations are dominant, the dynamical susceptibility shows a peak around q=0, thus, $1/T_1T$ is dominated by the component $\chi(q=0)$.

When the Knight shift and $1/T_1T$ arise from s electrons, the Korringa relation $1/T_1T$=constant is known to be satisfied. However, our data show that the T dependence of $1/T_1$ does not follow the simple Korringa relation. Here, we first discuss the spin fluctuations in these compounds at low temperatures in the framework of the modified Korringa relation. In general, the modified Korringa relation is written at low temperatures where the random-phase approximation is valid for spin fluctuations as

$$\frac{S_0}{T_1TK^2} = K(\alpha), \tag{4}$$

$$K(\alpha) \equiv \frac{(1-\alpha)^2}{\left[1-\alpha\dfrac{\chi_0(q)}{\chi_0}\right]_F^2}. \tag{5}$$

Here, $S_0 \equiv (\gamma_e/\gamma_n)^2(\hbar/4\pi k_B) = 3.88\times10^{-6}$ (sK) for ^{27}Al, where γ_e and γ_n are the electron and nuclear gyromagnetic ratios, respectively, α is the Stoner enhancement factor, χ_0 and $\chi_0(q)$ the static susceptibility and the q mode of the generalized susceptibility of noninteracting electrons, respectively, and $[\cdots]_F$ stands for the average over the Fermi surface. The ratio $K(\alpha)$ provides the important information on magnetic correlations. If $K(\alpha)<1$, the spin fluctuations are enhanced around q=0, leading to that the ferromagnetic correlations become significant. By using the experimental values of ^{27}K and $1/T_1T$, $K(\alpha)$ are estimated to be about 0.02 for x=0, 0.01, 0.02 and $K(\alpha)$=0.05 for x=0.05 and 0.1 at low temperatures. The values of $K(\alpha)$ are much smaller than 1, which evidences a predominance of ferromagnetic correlations for all the samples.

Next, we discuss the behavior of $1/T_1T$ at finite temperatures in the frame of the self-consistant renormalization (SCR) theory. The $1/T_1T$ can be obtained from Eq. (3) as

$$\frac{1}{T_1T} = \kappa_0\chi_d(T) + \beta \tag{6}$$

in the case when three-dimensional ferromagnetic fluctuations are dominant in the SCR theory,[8] where κ_0 is the coefficient written by spin-fluctuation parameters as explained later. Figure 8 shows the $1/T_1T$-χ plots for all the samples with temperature as an implicit parameter. The good linear relations were found between $1/T_1T$ and χ_d for all the samples at high temperatures, indicating that the ferromagnetic spin fluctuations possess three-dimensional characteristics in Ni_3AlC_x and can be quantitatively explained by the SCR theory. The relation $1/T_1T \propto \chi_d$ has been observed in some itinerant magnetic compounds, such as $Y(Co_{1-x}Al_x)_2$,[13,28] $Sr_{1-x}Ca_xRuO_3$,[29] and MnSi.[9]

As we will shown hereafter, the slope of the $1/T_1T$-χ plot not only includes the information of the energy scale of ferromagnetic spin fluctuations, that is T_0 but also the information of the hyperfine coupling constant A_{hf}. Because the hyperfine coupling constant show the carbon-component x dependence, it is necessary to eliminate the influence of A_{hf}^2 from $1/T_1T$ in order to obtain an insight into the influence of the carbon intercalation on the ferromagnetic spin fluctuations. For this propose, at first, we fit the $1/T_1T$-χ curve

shown in Fig. 8 with Eq. (6), and get the value of temperature-independent part of $1/T_1T$, β, from the intercept of the $1/T_1T$ axis. Although the temperature-independent part of magnetic susceptibility was thought to be considerably small for Ni_3Al,[25] here we can get the d-spin part susceptibility χ_d from the K-χ plot in Fig. 6 approximately. Then, we deduce the d-electron part $(1/T_1T)_d$. As a result, we get the $(1/T_1TA_{hf}^2)_d$-χ_d plot as shown in Fig. 9. The linear relationships are found between them in Fig. 9. Furthermore, we found that the slope of the line shows the large carbon-concentration dependence, which indicates that the carbon intercalation leads to the changes in the ferromagnetic spin-fluctuation spectrum in Ni_3AlC_x.

Consequently, from our NMR measurements, we found that the carbon intercalation modifies the electronic state near the Fermi surface, which leads to the changes in the hyperfine coupling constants A_{hf}, furthermore, the changes in the ferromagnetic spin-fluctuation spectrum in Ni_3AlC_x. In order to investigate how the ferromagnetic spin-fluctuation parameters are modified, the measurements of magnetic field dependence of T_1 are desired to be conducted.

IV. DISCUSSION

In this section, we show that the present spin-lattice relaxation results are interpreted in a quantitatively consistent way based on the framework of the SCR theory. Originally, the SCR theory was developed by Moriya and co-workers in order to interpret the nearly and weakly magnetism in the itinerant systems.[8] The dynamical susceptibility $\chi''(q,\omega)$ is characterized by two energy scales, T_0 and T_A, which correspond to magnetic spin fluctuations in energy ω and momentum q spaces, respectively. Using the parameters, T_0 and T_A, and some other parameters such as the mode-mode coupling constant $\bar{F}_1$, the Curie temperature T_C, and the spontaneous magnetization P_s and/or the $1/\chi_0$ at $T=0$, etc., the magnetic susceptibility can be calculated for weakly/nearly ferromagnetic materials according to the SCR theory.[30,31]

The parameters $\bar{F}_1$, T_C, P_s, and/or $1/\chi_0$, etc., can be deduced simply from the magnetization measurements, the problem is how to deduce the values of T_0 and T_A. Usually, T_0 can be obtained directly from the measurements of the nuclear spin-lattice relaxation rate $1/T_1$. According to the SCR theory, the linear relation between $(1/T_1T)$ and χ can be found, and the slope κ_0 of the $1/T_1T$-χ plot is written as

$$\kappa_0 = \frac{[\gamma_N A_{hf}(d)]^2 v_0}{4\pi^2 \Gamma_0 \mu_B}, \tag{7}$$

where Γ_0 characterizes the energy width of the dynamical spin-fluctuation spectrum. It always be transformed to the temperature scale as follows:

$$T_0 = \frac{\Gamma_0 q_B^3}{2\pi}, \tag{8}$$

where q_B is the effective zone-boundary vector given by $(6\pi^2/v_0)^{1/3}$ and v_0 the volume per magnetic atom. From the slope of the $1/T_1T$-χ plots, we get the values of κ_0. Using the A_{hf} obtained from the K-χ plot, we deduced the spin-fluctuation energy width T_0 for each sample as shown in Table II.

The most interesting feature of the concentration dependence of T_0 is that T_0 has a quite different value at the critical concentration $x\sim 0.02$ for the disappearance of the ferromagnetism, which corresponds to the discontinuous change in the hyperfine coupling constant A_{hf} at $x=0.02$. This behavior is quite different from the pressure-induced QCP in MnSi (Ref. 14) and the Ca-substitution-induced QCP in $Sr_{1-x}Ca_xRuO_3$,[29] where the T_0 decreases continuously as the system approaches to the QCP. The present results seem to be very similar to the $Y(Co_{1-x}Al_x)_2$ system, where the T_0 shows the divergence near the QCP because of the discontinuous change in the electronic state of $3d$ bands.[13] Similarly, our results suggest that the carbon intercalation leads to the discontinuous change in the Ni $3d$ electronic state at the critical concentration $x\sim 0.02$. The details are still unclear for the moment.

On the other hand, in order to get the value of T_A, the neutron-scattering experiments are needed. Unfortunately, it seems that there is no published data of T_A for these samples which can be used for our analysis. Therefore, we will discuss here for these samples by using the parameter value, $T_A=3.09\times 10^4$ K, estimated for Ni_3Al from the neutron-diffraction experiments.[32] Then we can calculate the inverse magnetic susceptibility for these samples with the following expressions:

TABLE II. Spin-fluctuation parameters of Ni_3AlC_x. The value of T_0 estimated from the NMR measurements and $\bar{F}_1$ were estimated from the slope of the Arrott plots. T_A were calculated from Eq. (7). T_A^* and $\bar{F}_1^*$ were determined from the simulations of the inverse magnetic susceptibilities as described in the text.

x	T_c (K)	T_0 (K)	T_A ($\times 10^4$ K)	T_A^* ($\times 10^4$ K)	$\bar{F}_1$ ($\times 10^5$ K)	$\bar{F}_1^*$ ($\times 10^5$ K)
0	36	3800	4.3	6.1	1.3	2.6
0.01	18	1700	3.2	4.3	1.6	2.9
0.02		4100	5.4	3.9	1.8	1.0
0.05		700	2.5	1.8	2.3	1.3
0.1		1000	3.4	3.7	3.0	3.7

$$\begin{cases} y \approx \bar{f}_1\left(-1 + \dfrac{1+\nu y}{c}\displaystyle\int_0^{1/\eta} dz z^3\left[\ln u - \dfrac{1}{2u} - \Psi(u)\right]\right), & \text{for weak ferromagnet,} \\ y = 1 + \eta K_0^2 \displaystyle\int_0^{1/K_0} dz z^3\left[\ln u - \dfrac{1}{2u} - \Psi(u)\right], & \text{for nearly ferromagnet.} \end{cases} \tag{9}$$

For weak ferromagnetic materials, $y^{-1}=4\eta^2 T_A\chi/3$, $u=z(y+z^2)/t$, $\eta=(T_C/T_0)^{1/3}$, $\bar{f}_1=\bar{F}_1 P_s^2/8T_A\eta^2$, $\nu=\eta^2 T_A/U$, $c=0.3353\ldots$, $t=T/T_C$, and U the intra-atomic exchange energy ($\sim 10^4$ K).[8,10,12] On the other hand, for nearly ferromagnetic metals, $y=\chi(0)/\chi$, $u=z(z^2+y)/t'$, $K_0^2=1/2\alpha T_A\chi(0)$, $\eta=15\bar{F}_1 T_0/2(\alpha T_A)^2$, and $t'=T/T^*$, $T^*=T_0K_0^3$.[31] Here $\Psi(u)$ is the digamma function. The calculated temperature dependence of the inverse susceptibility for Ni_3AlC_x is shown in Fig. 10(a) by solid lines. The agreements are fair at low temperatures.

Recently, Takahashi developed the SCR theory by assuming the conservation of the sum of the zero-point and thermal spin fluctuations, and deduced the relation between $\bar{F}_1$, T_A, and T_0 as[32,33]

$$\bar{F}_1 = \frac{4k_B T_A^2}{15T_0}, \tag{10}$$

which makes it possible to estimate the T_A from the magnetic measurements. Thus, we can obtain T_0 and T_A easily from the NMR and magnetic measurements without neutron-scattering data. Using the value of $\bar{F}_1$ reported previously,[19] we deduced T_A for each sample as shown in Table II. Using these parameters we calculated the inverse magnetic susceptibilities for Ni_3AlC_x numerically by Eq. (9) as shown in Fig. 10(a) with dotted lines. These results are quite close to the results calculated only by the SCR theory with the T_A value obtained for Ni_3Al and shown by the solid lines in Fig. 10(a).

Of course, the discrepancy between the experimental and the calculated results is found in the high-temperature range, which may be due to many assumptions. Here, we use Eq. (10) to modify our estimations of $\bar{F}_1$ and T_A. Then, we can get $\bar{F}_1^*$ and T_A^* which can give the best fit of the inverse magnetic susceptibilities as shown in Fig. 10(b) by solid lines. We succeed in obtaining very good agreements between experimental and calculated results as seen in Fig. 10(b). All the results are shown in Table II. For Ni_3Al, our results are two times larger than that had been reported. It may be because the T_C for our Ni_3Al is 36 K, which is a little lower than that used in the former calculation.[30] In our view, the values of T_A obtained by this method have the same order of magnitude compared with the values obtained experimentally, and can be considered reasonable.

In summary, though the C intercalation leads to the drastic changes in the magnetic ground state and the ferromagnetic spin-fluctuation spectrum, all the magnetic properties of Ni_3AlC_x from the ferromagnetic to paramagnetic states can be quantitatively understood by the SCR theory of spin fluctuations. Furthermore, the discontinuous change in the hyperfine coupling constant and T_0 may be connected with the QCP behavior at carbon concentration $x\sim 0.02$.

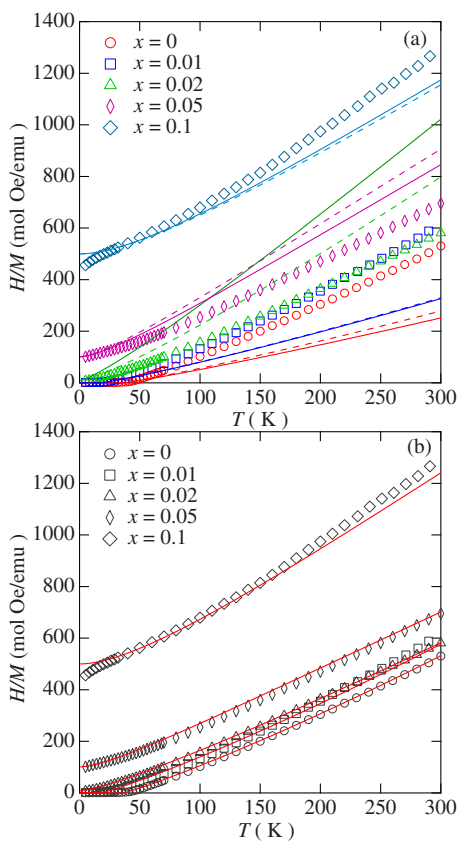

FIG. 10. (Color online) Simulation of temperature dependence of inverse magnetic susceptibilities (H/M) for Ni_3AlC_x (x=0, 0.01, 0.02, 0.05, and 0.1). (a) Dotted lines represent the calculated inverse magnetic susceptibilities based on the SCR theory with the parameters determined experimentally except T_A. Solid lines represent the simulation of H/M with the T_A deduced from Eq. (10) (b) Solid lines show the best-fitted lines for each samples (see text).

V. CONCLUSION

The magnetic properties of Ni_3AlC_x with x=0, 0.01, 0.02, 0.05, and 0.1 have been investigated by ^{27}Al NMR experiments from a microscopic point of view. We found that the magnitude of the negative ^{27}Al hyperfine coupling constant decreases first, and then increases monotonically with the increase in carbon concentration. The linear relationship between the $1/T_1T$ and the magnetic susceptibility χ indicates

the dominant of ferromagnetic correlations even in the case with paramagnetic Ni_3AlC_x. Using the parameters estimated from our experiments, we calculated the inverse magnetic susceptibilities. Quantitative good agreements can be successfully found between the experimental and the calculated H/M, implying that the rapid disappearance of ferromagnetic long-range ordering in Ni_3AlC_x should be regarded as three-dimensional ferromagnetic quantum phase transition, and that their magnetic characteristics including dynamical properties can be explained by the SCR and Takahashi theories of spin fluctuations in the Ni_3AlC_x system.

ACKNOWLEDGMENTS

This work was supported by a Grant-in-Aid for Science Research on Priority Area "Invention of Anomalous Quantum Materials" (Grant No. 16076210), and also by Global COE program, "International Center for Research and Advanced Education in Material Science," Kyoto University, from the Ministry of Education, Culture, Sports, Science and Technology of Japan. The present work was also supported by a Grant-in-Aid for Scientific Research (Grant No. 19350030) from the Japan Society for Promotion of Science.

*chenbin@kuchem.kyoto-u.ac.jp
†kyhv@kuchem.kyoto-u.ac.jp

[1] G. R. Stewart, Rev. Mod. Phys. **73**, 797 (2001).
[2] G. R. Stewart, Rev. Mod. Phys. **78**, 743 (2006).
[3] C. Pfleiderer, S. R. Julian, and G. G. Lonzarich, Nature (London) **414**, 427 (2001).
[4] P. G. Niklowitz, F. Beckers, G. G. Lonzarich, G. Knebel, B. Salce, J. Thomasson, N. Bernhoeft, D. Braithwaite, and J. Flouquet, Phys. Rev. B **72**, 024424 (2005).
[5] P. Pedrazzini, H. Wilhelm, D. Jaccard, T. Jarlborg, M. Schmidt, M. Hanfland, L. Akselrud, H. Q. Yuan, U. Schwarz, Y. Grin, and F. Steglich, Phys. Rev. Lett. **98**, 047204 (2007).
[6] D. A. Sokolov, M. C. Aronson, W. Gannon, and Z. Fisk, Phys. Rev. Lett. **96**, 116404 (2006).
[7] C. Pfleiderer, M. Uhlarz, S. M. Hayden, R. Vollmer, H. V. Lohenysen, N. R. Bernhoeft, and G. G. Lonzarich, Nature (London) **412**, 58 (2001).
[8] T. Moriya, *Spin Fluctuations in Itinerant Electron Magnetism* (Springer-Verlag, New York, 1985).
[9] M. Corti, F. Carbone, M. Filibian, Th. Jarlborg, A. A. Nugroho, and P. Carretta, Phys. Rev. B **75**, 115111 (2007).
[10] H. Ohta and K. Yoshimura, Phys. Rev. B **79**, 184407 (2009).
[11] Y. Ishikawa, Y. Noda, Y. J. Uemura, C. F. Majkrzak, and G. Shirane, Phys. Rev. B **31**, 5884 (1985).
[12] K. Yoshimura, M. Takigawa, Y. Takahashi, H. Yasuoka, and Y. Nakamura, J. Phys. Soc. Jpn. **56**, 1138 (1987).
[13] K. Yoshimura, M. Mekata, M. Takigawa, Y. Takahashi, and H. Yasuoka, Phys. Rev. B **37**, 3593 (1988).
[14] C. Thessieu, K. Kamishima, T. Goto, and G. Lapertot, J. Phys. Soc. Jpn. **67**, 3605 (1998).
[15] H. Sasakura, K. Suzuki, and Y. Masuda, J. Phys. Soc. Jpn. **53**, 754 (1984).
[16] M. Sato, J. Phys. Soc. Jpn. **39**, 98 (1975).
[17] T. Shinohara and T. Takasugi, J. Mater. Res. **8**, 1285 (1993).
[18] P. Tong, X. B. Zhu, B. C. Zhao, R. Ang, W. H. Song, and Y. P. Sun, Physica B **371**, 63 (2006).
[19] B. Chen, C. Michioka, Y. Itoh, and K. Yoshimura, J. Phys. Soc. Jpn. **77**, 103708 (2008).
[20] M. Sieberer, P. Mohn, and J. Redinger, Phys. Rev. B **75**, 024431 (2007).
[21] I. Hase, Mater. Trans. **47**, 475 (2006).
[22] F. R. de Boer, C. J. Schinkel, J. Biesterbos, and S. Proost, J. Appl. Phys. **40**, 1049 (1969).
[23] K. Suzuki and Y. Masuda, J. Phys. Soc. Jpn. **54**, 630 (1985).
[24] N. Buis, J. J. M. Franse, and P. E. Brommer, Physica B & C **106**, 1 (1981).
[25] T. Umemura and Y. Masuda, J. Phys. Soc. Jpn. **52**, 1439 (1983).
[26] *Metallic Shift in NMR*, edited by G. C. Carter, L. H. Bennett, and D. J. Kahan (Pergamon Press, Oxford, 1977).
[27] J. Owen and J. H. M. Thornley, Rep. Prog. Phys. **29**, 675 (1966).
[28] K. Yoshimura, T. Shimizu, M. Takigawa, H. Yasuoka, and Y. Nakamura, J. Phys. Soc. Jpn. **53**, 503 (1984).
[29] K. Yoshimura, T. Imai, T. Kiyama, K. R. Thurber, A. W. Hunt, and K. Kosuge, Phys. Rev. Lett. **83**, 4397 (1999).
[30] Y. Takahashi and T. Moriya, J. Phys. Soc. Jpn. **54**, 1592 (1985).
[31] R. Konno and T. Moriya, J. Phys. Soc. Jpn. **56**, 3270 (1987).
[32] Y. Takahashi, J. Phys. Soc. Jpn. **55**, 3553 (1986).
[33] Y. Takahashi, J. Phys.: Condens. Matter **13**, 6323 (2001).